

Electronic structure of $\text{PrBa}_2\text{Cu}_3\text{O}_7$

David J. Singh

Complex Systems Theory Branch, Naval Research Laboratory, Washington, D.C. 20375-5345

(Received 14 March 1994; revised manuscript received 15 April 1994)

Electronic-structure calculations, within the local spin density approximation (LSDA), are reported for $\text{PrBa}_2\text{Cu}_3\text{O}_7$. Significant charge transfer from the Pr ions to both the CuO_2 planes and the chains is found relative to $\text{YBa}_2\text{Cu}_3\text{O}_7$. This supports hole depletion explanations for the insulating character of $\text{PrBa}_2\text{Cu}_3\text{O}_7$. The LSDA electronic structure shows a prominent "ridge" Fermi surface analogous to that in $\text{YBa}_2\text{Cu}_3\text{O}_7$, but broader. It is proposed that high-resolution positron measurements of this width may provide a useful test of hole depletion models.

I. INTRODUCTION

It is remarkable that the Y ion in $\text{YBa}_2\text{Cu}_3\text{O}_7$ may be substituted by any rare-earth element except Ce, Tb, and Pr, with only minimal changes in the superconducting properties. Of the remaining three rare earths, only Pr forms single-phase compounds with the $\text{YBa}_2\text{Cu}_3\text{O}_7$ structure (1-2-3). Substitution of Pr for Y in $\text{Y}_{1-x}\text{Pr}_x\text{Ba}_2\text{Cu}_3\text{O}_7$ results in a rapid degradation of the superconducting properties, and an insulator with antiferromagnetically aligned Cu moments for large x .^{1,2} $\text{PrBa}_2\text{Cu}_3\text{O}_7$ is anomalous in other respects as well. For example, the Pr sublattice orders magnetically at 17 K, which is more than an order of magnitude higher than the ordering temperatures of other rare earths in the 1-2-3 structure. Despite a large body of theoretical and experimental work,² the understanding of $\text{PrBa}_2\text{Cu}_3\text{O}_7$ remains incomplete.

Initially, it was proposed, based on high-temperature susceptibility data showing an effective moment of approximately $2.7\mu_B$, that one hole per Pr was transferred from the CuO_2 planes relative to $\text{YBa}_2\text{Cu}_3\text{O}_7$ to form Pr^{4+} ions.³ This view is supported, for example (see Ref. 2 for a review), by optical and magnetic resonance experiments.^{4,5} It is interesting that $\text{PrBa}_2\text{Cu}_3\text{O}_7$ samples may contain excess oxygen while those of $\text{YBa}_2\text{Cu}_3\text{O}_7$ are generally oxygen deficient, although samples close to stoichiometry may be formed. This is significant, because of ionic considerations which imply that oxygen atoms bind electrons, thus providing holes to the rest of the crystal. The tendency of $\text{PrBa}_2\text{Cu}_3\text{O}_7$ to absorb more O than the corresponding Y system may then suggest a lower doping level in the Pr system. However, earlier band-structure calculations⁶ and other experimental studies⁷⁻¹⁰ imply the presence of Pr^{3+} ions, leading to the suggestion of a magnetic pair-breaking mechanism perhaps related to hybridization of the $4f$ levels with CuO_2 -derived states. Neither of these approaches has been shown to reconcile all the experimental data. Fehrenbacher and Rice¹¹ have proposed a hybrid model, in which holes are depleted from the CuO_2 planes, but the CuO chains and the Pr ions are mixed valent. In this picture, the insulating character of the material is explained as being due to extrinsic mechanisms such as de-

fects in the CuO chains that prevent them from conducting. This model is supported by light scattering⁵ and positron annihilation experiments,¹² which imply nonintegral band filling for the CuO chains.

Guo and Temmerman⁶ reported local spin density approximation (LSDA) electronic-structure and total-energy calculations for $\text{PrBa}_2\text{Cu}_3\text{O}_7$ with the Pr f orbitals constrained to integer occupations of one and two electrons. These calculations, which were performed using the linearized muffin-tin-orbital method within the atomic-sphere approximation (LMTO-ASA), yielded lower total energies for a doubly occupied $4f$ shell than for the singly occupied case. That is, they found that trivalent Pr yielded a lower total energy, and concluded that Pr is trivalent in $\text{PrBa}_2\text{Cu}_3\text{O}_7$. Since trivalent Pr means that the Pr is not effective in depleting holes from the CuO_2 layers, Guo and Temmerman ascribed the non-superconducting character of $\text{PrBa}_2\text{Cu}_3\text{O}_7$ to a magnetic pair-breaking effect.

Here, LSDA calculations performed with a local orbital extension¹² of the general potential linearized augmented-plane-wave (LAPW) method¹³⁻¹⁵ are reported. This method avoids shape approximations to the charge density or potential and is therefore well suited to treating materials with open structures and low site symmetries, such as the superconducting cuprates. Additionally, the local orbital extension permits an accurate treatment of high-lying extended core states, such as the $5p$ state of Pr. The f orbitals were treated as valence states, thus permitting nonintegral occupations. These features permit a detailed determination of the LSDA electronic structure of $\text{PrBa}_2\text{Cu}_3\text{O}_7$, and in particular a precise determination of the position and shape of the "ridge" Fermi-surface section; this may then be compared with the measured size and shape from positron angular correlation of annihilation radiation (ACAR) experiments and compared with previous calculations for $\text{YBa}_2\text{Cu}_3\text{O}_7$.¹⁶⁻¹⁸ This also permits a more detailed study of the Pr valence and any transfer of holes from the CuO_2 layers.

II. COMPUTATIONAL APPROACH

As mentioned, the present calculations were performed within the LSDA using a local orbital extension of the

general potential LAPW method. Since this method has been reviewed in detail elsewhere,^{14,15} only aspects specific to the present calculation are discussed here. The calculations were performed for stoichiometric $\text{PrBa}_2\text{Cu}_3\text{O}_7$ using the experimental crystal structure.¹⁹ The Hedin-Lundqvist²⁰ parametrization of the LSDA was used with the spin scaling of von Barth and Hedin.²¹ Both the core and valence states were treated self-consistently, the core states relativistically in an atomic-like approximation and the valence states scalar relativistically, with spin-orbit interactions added in a second variational step. A well-converged basis set consisting of approximately 1550 functions was used. Self-consistency was obtained using a set of 16 special \mathbf{k} points²² in the irreducible wedge of the Brillouin zone (IBZ). This is expected to be adequate for the present purpose of obtaining an understanding of the charge balance between various parts of the crystal and the corresponding effects on the electronic structure. The electronic density of states (DOS) and Fermi surfaces were obtained from eigenvalues calculated at 96 uniformly distributed \mathbf{k} points in the IBZ.

III. NON-SPIN-POLARIZED ELECTRONIC STRUCTURE

The non-spin-polarized relativistic (including spin-orbit interaction) band structure and corresponding total and projected DOS of $\text{PrBa}_2\text{Cu}_3\text{O}_7$ are shown in Figs. 1 and 2, respectively. The band structure is qualitatively similar to that of $\text{YBa}_2\text{Cu}_3\text{O}_7$ with the addition of a manifold of Pr f -derived bands near the Fermi energy (E_F). The Pr f bands are centered approximately 0.3 eV above E_F . Some hybridization between the valence states and the f bands is evident in the calculations, as shown by the distortions of the remaining bands as they cross the f -band region. Because of this it is difficult to precisely define the f -band width. Taking it as the width of the Pr f component of the DOS at 40 Ry^{-1} , a value of 0.95 eV results. Not surprisingly, chain-derived bands are least

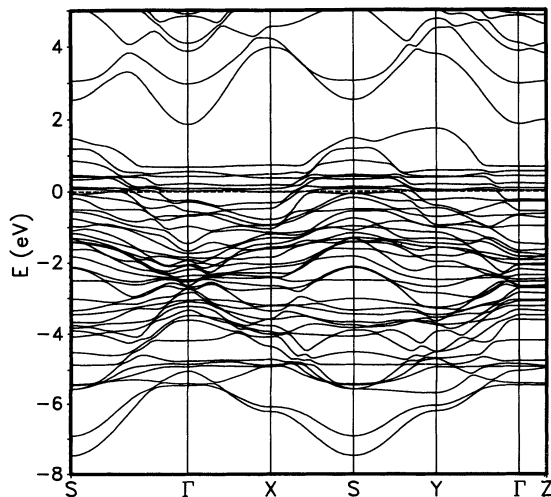


FIG. 1. Non-spin-polarized band structure of $\text{PrBa}_2\text{Cu}_3\text{O}_7$. The dashed horizontal line denotes the Fermi energy.

affected by hybridization with the f bands. This non-spin-polarized calculation shows only a small f -band contribution below E_F , amounting to somewhat more than one electron but clearly less than two electrons per cell. There is noticeably less dispersion in the z -axis direction relative to $\text{YBa}_2\text{Cu}_3\text{O}_7$, particularly near E_F . This reflects reduced hybridization between plane- and chain-derived bands, which is also reflected in the Fermi surfaces.

The calculated non-spin-polarized Fermi surfaces are shown in Fig. 3. Although there are large differences from the Fermi surfaces of $\text{YBa}_2\text{Cu}_3\text{O}_7$,¹⁶⁻¹⁸ due to hybridization with the Pr f bands, some similarities remain. In particular, the chain-related “ridge” section, although shifted, remains intact. The electron-containing “ridge” feature is broadened by this shift, resulting in an increase of about $\frac{1}{2}$ in its charge. The small S - R -centered hole cylinder, present in $\text{YBa}_2\text{Cu}_3\text{O}_7$, is absent in Fig. 3. The band that gives rise to it is, however, evident in the band structure, approaching E_F from below but not reaching

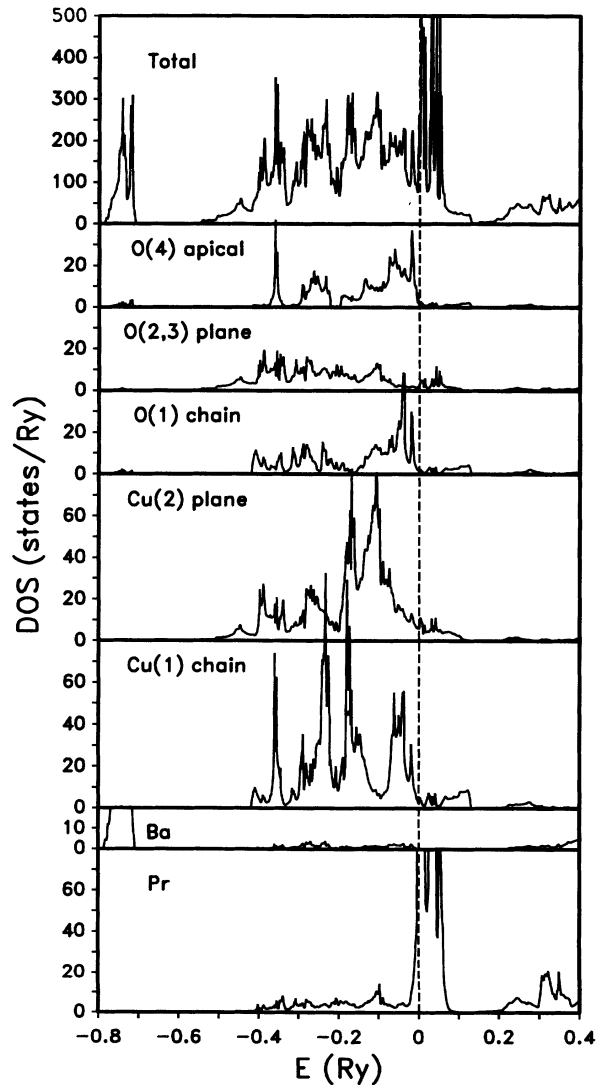


FIG. 2. Total and projected electronic DOS of $\text{PrBa}_2\text{Cu}_3\text{O}_7$ from non-spin-polarized calculations. The dashed vertical line denotes the Fermi energy.

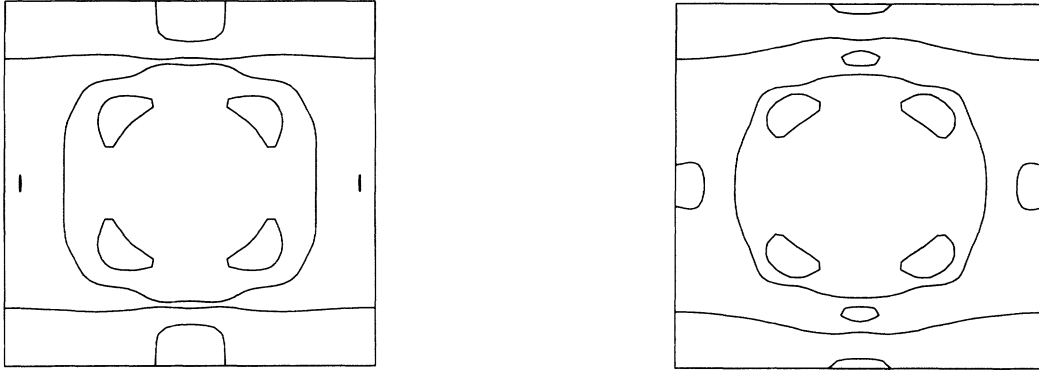


FIG. 3. Fermi surfaces in the $k_z=0$ plane (left) and $k_z=\frac{1}{2}$ planes (right) for $\text{PrBa}_2\text{Cu}_3\text{O}_7$ from non-spin-polarized calculations. The Γ (Z) points are at the corners, the S (R) point in the center, the X (U) points at the midpoints of the horizontal edges, and the Y (T) points at the midpoints of the vertical edges.

E_F . It is unclear whether this is due to hybridization with f bands or a shift in the band, although the latter is consistent with the broadening of the “ridge.” In any case, the shift in the “ridge” section implies that the chains are providing even more hole doping in $\text{PrBa}_2\text{Cu}_3\text{O}_7$ than in $\text{YBa}_2\text{Cu}_3\text{O}_7$. The outer “barrel” section, which is essentially (there is some mixing depending on the \mathbf{k} point) odd with respect to reflection in the plane containing the Pr atom, is also relatively unperturbed. The inner “barrel” section hybridizes more strongly with the f bands near E_F and is not clearly shown in Fig. 3. The band that gives rise to the inner “barrel” section can, however, be seen crossing through and hybridizing with the f bands in Fig. 1. The outer hole-containing “barrel” is smaller than the corresponding Fermi surface in $\text{YBa}_2\text{Cu}_3\text{O}_7$, indicating a transfer of holes out of the CuO_2 planes as well as out of the chains. This is consistent with the fact that only about one f electron occurs below E_F in the DOS (assignment of a precise number is complicated by the hybridization present in this energy range).

Another view of this charge transfer may be gained by examining the Fermi surfaces that would result in the absence of hybridization with the f bands. This may be done by computing eigenvalues and band characters on a grid of \mathbf{k} points in the Brillouin zone, and then identifying those for which there are Cu-O-derived bands with substantial f hybridizations. These \mathbf{k} points may then be eliminated from the data set and replaced by interpolated bands from other \mathbf{k} points with the f bands discarded. In the present case, the criterion used was to discard \mathbf{k} points for which there were not 14 f bands all with more than 70% f character. This led to the removal of $\frac{1}{4}$ of the \mathbf{k} points. The Fermi surfaces (keeping the same E_F) for the resulting interpolated bands are shown in Fig. 4. These Fermi surfaces are more clearly related to those of $\text{YBa}_2\text{Cu}_3\text{O}_7$. The “ridge” section is somewhat changed from that of Fig. 3, reflecting the removal of hybridization with the f bands, but is still significantly broader (by approximately 25%) than that in $\text{YBa}_2\text{Cu}_3\text{O}_7$. The two “barrels” show less interaction with the ridge and are closer together. Significantly, the area of the barrels is

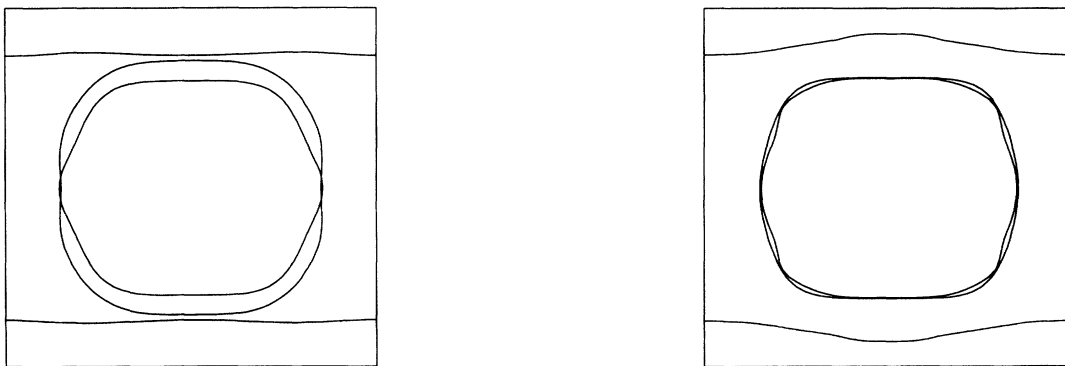


FIG. 4. Cu-O component (see text) of the Fermi surfaces in the $k_z=0$ plane (left) and $k_z=\frac{1}{2}$ planes (right) for $\text{PrBa}_2\text{Cu}_3\text{O}_7$ from non-spin-polarized calculations. The Γ (Z) points are at the corners, the S (R) point in the center, the X (U) points at the midpoints of the horizontal edges, and the Y (T) points at the midpoints of the vertical edges.

noticeably smaller than that in $\text{YBa}_2\text{Cu}_3\text{O}_7$, supporting the earlier conclusion that the doping level is strongly reduced in $\text{PrBa}_2\text{Cu}_3\text{O}_7$ and that the “ridge” is broadened.

IV. SPIN-POLARIZED ELECTRONIC STRUCTURE

The Pr ions in $\text{PrBa}_2\text{Cu}_3\text{O}_7$ are clearly magnetic as evidenced by the antiferromagnetic ordering of these moments at low temperatures. Further, spin polarization of the f orbitals in lanthanides can have a substantial effect on the energetics. Therefore it is important to determine to what extent the results of the previous section may be altered by magnetic effects on the Pr ions. Spin-polarized calculations, within the LSDA, were used to study this issue. Since magnetic ordering of the Pr ions is expected to contribute only a small energy relative to the band energies and therefore not significantly affect the charge balance between the various components of the crystal, a

ferromagnetic ordering was used rather than the experimentally observed antiferromagnetic ordering. Fixed-spin-moment calculations^{23,24} were performed for several magnetizations between zero and $2.3 \mu_B/\text{cell}$ as well as unconstrained calculations. Only one stable magnetic solution was found. This ferromagnetic solution had a total energy 11 mRy/cell lower than the non-spin-polarized solution, and a spin magnetization of $1.1 \mu_B/\text{cell}$. The electronic DOS is shown in Fig. 5. Little change is evident from the non-spin-polarized DOS, except with regard to the Pr-derived electronic structure. The main differences are a small increase in f occupation and an exchange splitting of the f bands. Within these LSDA calculations, the exchange splitting of the f bands is 0.94 eV. Applying the same criterion as for the non-spin-polarized f -band width, a majority-spin f -band width of approximately 0.8 eV is obtained; this is slightly narrower than the non-spin-polarized f -band width.

The wave functions within the Pr sphere (radius 2.4 a.u.) contribute a spin magnetization of $1.4 \mu_B/\text{Pr atom}$, while the remaining atoms show small reverse polarizations. Since the minority-spin f bands are entirely above E_F this can be used to estimate the f occupation as 1.4 electrons. Thus these calculations imply a Pr valence intermediate between Pr^{4+} and Pr^{3+} . The total charge in the Pr LAPW sphere differs from the non-spin-polarized calculation by only 0.01 electrons. The Fermi surfaces, shown in Fig. 6, are complicated by distortions due to hybridization with the majority-spin f bands near E_F . Nonetheless, “barrel” and “ridge” sections remain identifiable and the small chain-derived hole section around S , which was absent in the non-spin-polarized calculation, reappears. The k -space dispersion of this Fermi surface arises from a small exchange splitting of 0.02 eV combined with the flatness of this band near the maximum at S . The reappearance of this section implies that the Pr is less effective in depleting holes from the chains in the spin-polarized than in the non-spin-polarized calculations. Nonetheless the ridge section remains broader than in $\text{YBa}_2\text{Cu}_3\text{O}_7$.

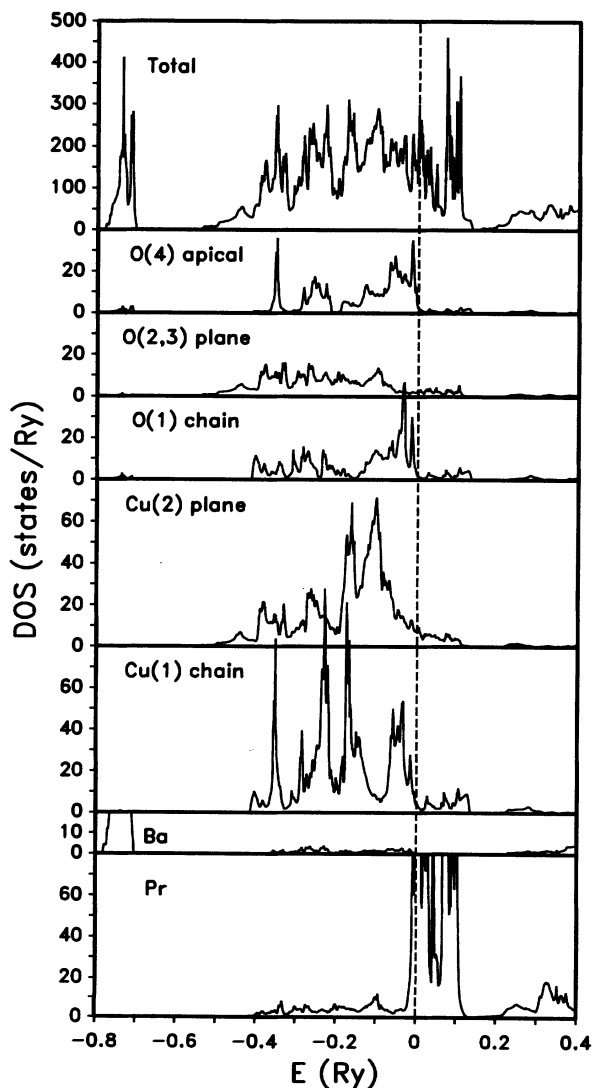


FIG. 5. Total and projected electronic DOS of ferromagnetic $\text{PrBa}_2\text{Cu}_3\text{O}_7$. The dashed vertical lines denote the Fermi energy.

V. CONCLUSIONS

LSDA calculations for $\text{PrBa}_2\text{Cu}_3\text{O}_7$ have been performed. These calculations show a substantial charge transfer from the Pr ions relative to the Y ions in $\text{YBa}_2\text{Cu}_3\text{O}_7$, and are consistent with models like that of Fehrenbacher and Rice, which ascribe the insulating character of $\text{PrBa}_2\text{Cu}_3\text{O}_7$ to hole depletion in the CuO_2 planes. Using the calculated Pr spin moment, I estimate the transfer within the LSDA to be 0.6 holes/Pr atom, distributed between the chains and planes. Although the plane-derived electronic structure near E_F is strongly perturbed, the chain-derived “ridge” Fermi surface remains evident. The width of the ridge is increased relative to $\text{YBa}_2\text{Cu}_3\text{O}_7$, reflecting a depletion of “holes” (increase in number of electrons) in both the CuO_2 planes and in the chains. This hole depletion may be viewed equivalently as an increase in the Fermi energy for the non-Pr electronic structure with some additional shifts between the various bands. It is notable that experimen-

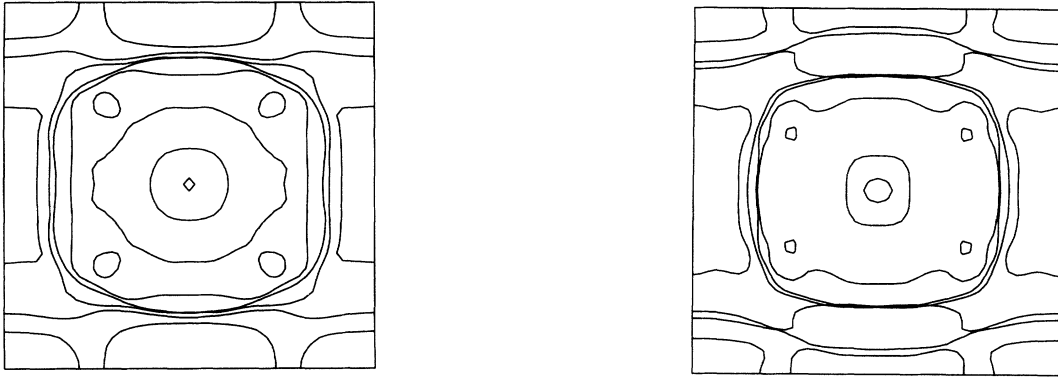


FIG. 6. Fermi surfaces in the $k_z = 0$ plane (left) and $k_z = \frac{1}{2}$ planes (right) for $\text{PrBa}_2\text{Cu}_3\text{O}_7$ from spin-polarized calculations. The Γ (Z) points are at the corners, the S (R) point in the center, the X (U) points at the midpoints of the horizontal edges, and the Y (T) points at the midpoints of the vertical edges.

tal studies of $(\text{Y}_{1-x}\text{Pr}_x)\text{Ba}_2\text{Cu}_4\text{O}_8$ find that Pr is less effective in suppressing superconductivity,²⁵ even though the local structure and the CuO_2 -plane-derived electronic structures are similar to those of the $(\text{Y}_{1-x}\text{Pr}_x)\text{Ba}_2\text{Cu}_3\text{O}_7$ system. The present calculations suggest an explanation in terms of the additional CuO unit in this material, which could provide additional holes and make depletion of those in the CuO_2 planes more difficult. These calculations are, however, subject to the limitations of the LSDA, such as its inability to correctly describe the antiferromagnetic insulating CuO_2 planes in undoped high- T_c materials; these may affect the amount of the charge transfer. High-resolution positron ACAR measurements of the width of the “ridge” section will be very useful in determining whether this in fact occurs in real

$\text{PrBa}_2\text{Cu}_3\text{O}_7$. The present calculations strongly suggest a hole depletion explanation for the insulating character of this material. Positron experiments, if they find an increased “ridge” width relative to $\text{YBa}_2\text{Cu}_3\text{O}_7$, will further support this picture.

ACKNOWLEDGMENTS

I am pleased to acknowledge several helpful discussions with M. Osofsky and W. E. Pickett. I am grateful to L. Hoffmann and B. Barbiellini for a prepublication copy of Ref. 12. Work at the Naval Research Laboratory is supported by the Office of Naval Research. Computations were performed at the Cornell National Supercomputer Facility.

- ¹L. Soderholm, K. Zhang, D. G. Hinks, M. A. Beno, J. D. Jorgenson, C. U. Segre, and I. K. Schuller, *Nature* **328**, 604 (1987).
- ²H. B. Radousky, *J. Mater. Res.* **7**, 1917 (1992), and references therein.
- ³Y. Dalichaouch, M. S. Torikachvili, E. A. Early, B. W. Lee, C. L. Seaman, K. N. Yang, H. Zhou, and M. B. Maple, *Solid State Commun.* **65**, 1001 (1988).
- ⁴A. P. Reyes, D. E. MacLaughlin, M. Takigawa, P. C. Hammel, R. H. Heffner, J. D. Thompson, and J. E. Crow, *Phys. Rev. B* **43**, 2989 (1991).
- ⁵K. Takenaka, Y. Imanaka, K. Tamasaku, T. Ito, and S. Uchida, *Phys. Rev. B* **46**, 5833 (1992).
- ⁶G. Y. Guo and W. M. Temmerman, *Phys. Rev. B* **41**, 6372 (1990).
- ⁷U. Neukirch, C. T. Simmons, D. Sladeczek, C. Laubschat, O. Strelbel, G. Kaindl, and D. D. Sarma, *Europhys. Lett.* **5**, 567 (1988).
- ⁸J. S. Kang, J. W. Allen, Z. X. Shen, W. P. Ellis, J. J. Yeh, B. W. Lee, M. B. Maple, W. E. Spicer, and L. Lindau, *J. Less-Common Met.* **148**, 121 (1989).
- ⁹J. Fink, N. Nucker, H. Romberg, M. Alexander, M. B. Maple, J. J. Neumeier, and J. W. Allen, *Phys. Rev. B* **42**, 4823 (1990).
- ¹⁰G. Hilscher, E. Holland-Moritz, T. Holubar, H. D. Jostardt, V. Nekvasil, G. Schaudy, U. Walter, and G. Fillion, *Phys. Rev. B* **49**, 535 (1994).
- ¹¹R. Fehrenbacher and T. M. Rice, *Phys. Rev. Lett.* **70**, 3471 (1993).
- ¹²L. Hoffmann, A. A. Manuel, M. Peter, E. Walker, M. Gauthier, A. Shukla, B. Barbiellini, S. Massidda, G. Adam, S. Adam, W. N. Hardy, and R. Liang, *Phys. Rev. Lett.* **71**, 4047 (1993).
- ¹³D. Singh, *Phys. Rev. B* **43**, 6388 (1991).
- ¹⁴O. K. Andersen, *Phys. Rev. B* **12**, 3060 (1975).
- ¹⁵S. H. Wei and H. Krakauer, *Phys. Rev. Lett.* **55**, 1200 (1985); D. J. Singh, *Planewaves, Pseudopotentials and the LAPW Method* (Kluwer, Boston, 1994), and references therein.
- ¹⁶W. E. Pickett, R. E. Cohen, and H. Krakauer, *Phys. Rev. B* **42**, 8764 (1990); H. Krakauer, W. E. Pickett, and R. E. Cohen, *J. Supercond.* **1**, 111 (1988); W. E. Pickett, H. Krakauer, R. E. Cohen, and D. J. Singh, *Science* **255**, 46 (1992).
- ¹⁷J. Yu, S. Massidda, A. J. Freeman, and D. D. Koelling, *Phys. Lett. A* **122**, 203 (1987).
- ¹⁸O. K. Andersen, O. Jepsen, A. I. Liechtenstein, and I. I. Mazin, *Phys. Rev. B* **49**, 4145 (1994); C. O. Rodriguez, A. I. Liechtenstein, I. I. Mazin, O. Jepsen, O. K. Andersen, and M. Methfessel, *ibid.* **42**, 2692 (1990).
- ¹⁹J. J. Neumeier, T. Bjornholm, M. B. Maple, J. J. Rhyne, and

- J. A. Gotaas, *Physica C* **166**, 191 (1990).
- ²⁰L. Hedin and B. I. Lundqvist, *J. Phys. C* **4**, 2064 (1971).
- ²¹U. von Barth and L. Hedin, *J. Phys. C* **5**, 1629 (1972).
- ²²A. Baldereschi, *Phys. Rev. B* **7**, 5212 (1973); H. J. Monkhorst and J. D. Pack, *ibid.* **13**, 5188 (1976).
- ²³K. Schwarz and P. Mohn, *J. Phys. F* **14**, L129 (1984); see also A. R. Williams, V. L. Moruzzi, J. Kubler, and K. Schwarz, *Bull. Am. Phys. Soc.* **29**, 278 (1984).
- ²⁴D. J. Singh and J. Ashkenazi [*Phys. Rev. B* **46**, 11 570 (1992)] discuss the inclusion of spin-orbit interaction in this procedure.
- ²⁵Z. Guo, N. Yamada, K. I. Gondaira, T. Iri, and K. Kohn, *Physica C* **220**, 41 (1994).